Li, S, Al-Badani, K, Gu, Y, Lake, MJ, Li, B, Rothwell, G and Ren, X

The Effects of Poisson's Ratio on the Indentation Behaviour of Materials with Embedded System in an Elastic Matrix

The Effects of Poisson's Ratio on the Indentation Behaviour of Materials with Embedded System in an Elastic Matrix

Shudong Li[1], Khaled Al-Badani[1], Yaodong Gu[2], Mark Lake[3], Lisa Li[1], Glynn Rothwell[1] and James Ren[1*]

[1] Faculty of Technology and Engineering, Liverpool John Moores University, Liverpool, UK
[2] Faculty of Sports Science, Ningbo University, Ningbo 315211, China
[3] School of Sport and Exercise Sciences, Faculty of Science, Liverpool John Moores University, Liverpool, UK

Keywords Embedded Shell, Indentation, Auxeticity, Indentation Stiffness/Resistance .

Abstract: Soft materials with an embedded stiffer layer are increasingly used in medical and sports engineering. A detailed understanding of the mechanical behaviour of such a material system under localised load and resistance to indentation is very important. In this work, the deformation of an isotropic soft matrix with a buried stiffer thin layer under a circular flat indenter was investigated through finite element (FE) modelling. A practical approach in simulating the indentation resistance of such a system (soft matrix with a buried thin stiffer layer) is evaluated. The numerical result is correlated with the data based on analytical approaches for both homogenous materials and elastic half space with an embedded stiffer layer. The influence of Poisson's ratio and auxeticity of the matrix on the deformation and indentation stiffness of the material system under different conditions (indenter size, sheet thickness and embedment depth) were established and main influences of the Poisson's ratio on the material deformation and stresses are discussed. The result shows that the influence of matrix auxeticity on indentation resistance is highly depth dependent, with over 30% enhancement of the indentation resistance being predicted for materials with matrix of a negative Poisson's ratio.

1 Introduction

Soft materials, with embedded thin stiffer layers (i.e. the in-plane dimension is much larger than the thickness), are increasingly being used in many products particularly within medical and sports engineering fields, such as embedded sensors, heating elements and various other applications [1-3]. The materials are also directly relevant to development in smart or multifunctional elastomeric materials for sensors, stretchable electronics, etc. [3]. In many cases, the embedded/inserted structure has a much larger in-plane dimension than its thickness, and the material system may consist of embedment of different thickness and depth from the surface of embedment in different matrix materials (e.g. rubber, soft plastics, foams). Based on the relative material properties between the embedment and the matrix, one type can be termed rigid/inextensible inserts with the embedment having a much higher stiffness than the matrix. Typical cases included embedded electrical sensors (e.g. thin Piezoelectric sensor of a thin copper sheet with ceramic coating and thin film thermocouples [3]), where the stiffness of these metals/ceramics coating is much higher than the matrix (typically silicone rubber/gel). Another type, which can be termed as deformable inserts, have a relatively softer insert embedded in silicone rubber. Typical examples include plastic inserts in silicone rubber for insoles or orthotics. A detailed fundamental understanding of the mechanical behaviour of these material systems, under different loading conditions is crucial to the structural integrity of the system, functional performance of the embedment, as well as the reliability of these products. For example, a rubber based matrix is required to provide protection as well as flexibility under different loading conditions. One critical loading condition is indentation, which could cause damage to the matrix and the inserts resulting in malfunction. Therefore, it is important to understand the effects of the matrix properties and the key design parameters, such as depth of the embedment from the sample surface, on the indentation resistance, compliance and deformation of the system.

Most of relevant early work on indentation of material systems reinforced with a single stiffer layer has been focused on theoretical work for the understanding of mechanics related to geomechanics and foundation engineering due to the large relative in-plane dimension and thickness ratio of the layers in these material systems [4-9]. Selvadurai [4] studied the problem of the axisymmetric Boussinesq–Sneddon–Harding indentation problem for an isotropic elastic half space reinforced with an inextensible membrane that is placed at a finite depth from the surface. The work provided results illustrating the influence of the embedded depth of the embedment and the effect of the Poisson's ratio on indentation resistance of the system. Eskandari et al [7] studied the lateral translation of an inextensible circular membrane embedded in a transversely isotropic half-space. The study demonstrated that the lateral stiffness of an embedded inextensible circular membrane is highly dependent on the embedment depth and the Poisson's ratio of the matrix. Recently, Shodja et al [8] investigated the indentation process of a transversely isotropic half-space, which is reinforced by a buried inextensible membrane. The investigation established the effects of anisotropy, embedment depth of the membrane, and material incompressibility on both the contact stress and the normal stiffness factor. All of these studies highlighted the importance of the Poisson' ratio effect and depth of the shell in the mechanical behaviour of a material system with embedded thin stiffer layer under localised loading. It is of great interest to systematically investigate the effect of the Poisson's ratio in particular auxeticity [10-15] on the indentation behaviour of such a system. Materials with negative Poisson's ratio have been the topic of research and development for several decades [16-21]. The material expands transversally upon being stretched and shrinks under compression. Many different mechanisms have been designed and explored, which has opened up more opportunities to develop negative Poisson's ratio materials at different length scales, in some cases, the material can be treated as a homogenous system [22–30].

It is well documented that, negative Poisson's ratio influences the material deformation under localised deformation such as indentation [31-33]. Most of the earlier work has been focused on foam structures, while recent investigation/predictions on the isotropic auxetic materials have increased with the development of new auxetic material systems at different scales [34-38]. A recent study performed by Argatov et al [37] investigated indentation and impact compliance of isotropic auxetic materials from the continuum mechanics viewpoint, the effect of Poisson's ratio and auxeticity is found to be dependent on the shape of the indenter, a stronger effect of Poisson's ratio for a flat ended indenter than that for a spherical indenter is predicted. Furthermore, Photiou et al [33] illustrated via theory and numerical modelling, that the negative Poisson's ratio has much stronger influence on the normalised hardness than the positive Poisson's ratio. The work also shows that evolution of different material constants (E, G, K) as a function of Poisson's ratio follow a different trend over the positive to negative domains. In a study on thin membranes with fixed boundary conditions [38], which is a situation also relevant to the embedded thin membranes; it is highlighted that negative Poisson's ratios have direct influence on the deformation, the force–displacement curve, the deflection profile and the contact area. It should be noted that when a thin membrane/shell is embedded in a matrix, the deformation of the system (matrix and embedment) under localised/pointed deformation (indentation) is much more complex due to the combined interaction from the matrix, the shell properties and the depth of the shell under the indenter. Hence, a systematic investigation is required to investigate the deformation of the material system and factors affecting the indentation resistance/stiffness, which are critical factors for the design and application of such systems as well as developing new material systems.

In this work, the deformation of an embedded stiffer layer in a softer matrix under a circular flat indenter, was investigated through FE modelling. A practical approach in modelling embedded thin layers is evaluated and established. The numerical data is correlated with results based on analytical approaches for homogenous materials and material with an embedded inextensible thin layer. The indentation stiffness/resistance of the material system, with a thin

stiffer layer and a matrix of positive or negative Poisson's ratio values were systematically studied. The influence of auxeticity on the force-indentation depth data and deformation of the system under different conditions (indenter size, sheet thickness and embedment depth) was established and the effects of the Poisson's ratio are discussed.

2. Modelling approach and validation

2.1 Modelling approach

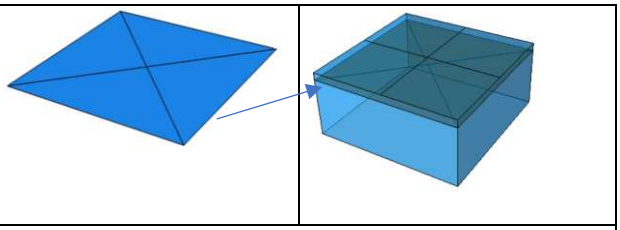

Figure 1 Material system with an embedded stiffer layer in a homogenous matrix.

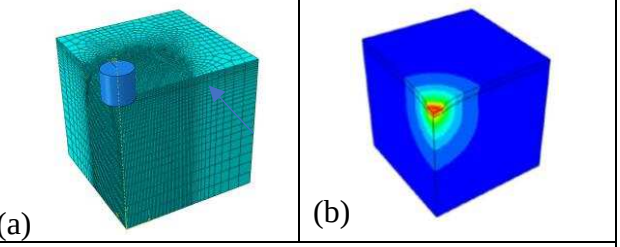

Figure 2 Typical FE model/mesh (a) and deformation field (b).

Figures 1&2 show the structure and FE model with a thin stiffer layer embedded in a homogenous matrix. The FE model is developed using the explicit code in Simulia ABAQUS (version 6.14) [39]. The radius of the indenter is 1 or 2 mm. The sample is at least 10 times the indenter radius to avoid sample size effect. As shown in the figure, a thin shell is built, and then embedded in a square block sample (40x40x20mm). The indenter is modelled as a rigid body as it is much stiffer than the sample. The embedded layer is modelled by a finite-strain shell element S4R with 5 integration points. The matrix is modelled by C3D8 elements. The procedure used constraint type of "Embedded Region" to model the interaction between the thin layer within the "whole model" [39]. This approach allows the user to insert a structure within a "host" region of the model or within the whole model [39]. The matrix is the host elements while the shell elements of the embedment was treated as the embedded elements. A standard Weightfactor round off tolerance (1E-06) is used. During the FE model development stage, a range of shell thicknesses have been used (0.1-1mm). With this procedure, the position and thickness of the shell can be modified within the system without the need of changing the meshing of the matrix. Using such an approach, the model can be modified flexibly through parametric studies to simulate indentation tests of different situations, such as sample size, indenter size, shell thickness, position of the shell from the surface, mechanical properties of the shell and matrix, etc. In the FE model, the bottom face of the sample is fixed on all degrees of freedom (DOFs.), the displacement of the indenter is controlled by the applied velocity and the total time.

Three conditions have been investigated to establish the validity of the model and to investigate the effect of key material and dimensional parameters on the indentation process. The first

model (Designated as the Homogenous model) is a model with no thin shell embedded, this allows a direct comparison between the numerical results and known analytical solutions for indentation of an elastic half space with a circular flat-ended indenter. The second model (Designated as the inextensible shell model) consists of a sample with an embedded shell, which is much stiffer than the matrix (in this case, E_s is over 100 times that of E_m). The third model is similar to the inextensible model, but in this case, a shell with lower stiffness is used. This model is designated as the "deformable shell model". The flat-ended cylindrical indenter is modelled as a rigid material with a changeable indenter size, the majority of the results presented is based on data for indenter radius of 1 or 2mm, as they are more relevant to situations where a sharper object poses more problems to embedded systems. A fixed displacement is applied on the indenter to move it onto the sample, with no rotation or lateral movement being allowed. The results reported in this work are based on a quarter symmetric model. Mesh sensitive tests have been performed by changing the element size in the model until there is no significant change of the modelling results (force within 2%) with mesh size. In the presented case, the matrix is modelled with over 20000 elements and the embedded shell is modelled with 1845 shell elements. A parametric program (ABAQUS-Plugin, Explicit) has been developed, which can alter various key elements within the 3D model, such as the indenter/sample size, thickness, material properties and the position of the embedded shell. The stiffness (E_m) is fixed at 3MPa, the effect of the matrix Poisson's ratio is investigated systematically, by changing its value between -0.5 and 0.5.

2.2 Validation against analytical approaches.

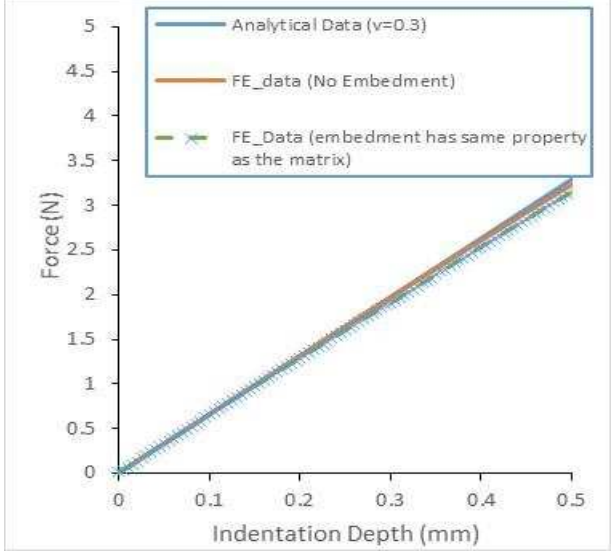

Figure 3 Comparison between FE indentation force-displacement data for a homogeneous matrix (i.e. no Embedment) and an FE model with an embedded layer having the same properties as the matrix against analytical data for indentation of a homogenous sample with a cylindrical indenter.

Figure 3 shows a typical data comparing the results from two modelling conditions against the analytical data based on the equation for a homogeneous sample (Equation 1). One FE data is for the model without embedded shell, the other FE data is for the sample with an embedded shell, in which the shell has the same material properties as the matrix. In both cases, the two FE data (one is with shell and one is without embedded shell) are in good agreement with the analytical solution (Equation 1) for flat-ended cylindrical indentation on a homogeneous material [40].

$$P = \frac{2bE\Delta}{(1-v^2)} \quad (1)$$

Where 'P' is the load on the indenter, 'b' is the radius of the cylindrical indenter; 'E' is the Young's Modulus of the matrix. 'v' is the Poisson's ratio of the matrix. 'Δ' is the displacement of the indenter. For the data presented in Figure 3, the Young's Modulus used is 3MPa, and the Poisson's ratio is 0.3. A similar level of agreement could be found in other material properties or shell depth combinations. The close agreement between the homogenous model and the FE model with embedded shell of the same material property, shows that the modelling approach using an "Embedded Region" in the interaction module is sufficiently accurate. In the preliminary investigation, a full solid model has been developed in which the shell is modelled by solid elements, the results are similar (within 5%) but a very fine mesh is required due to large ratio of the in-plane and out-of-plane dimension of the embedded layers, which cause a much higher demand on the computational resource and time than the "embedded region" approach. In all cases, the force and displacement follows a linear relationship. The force-displacement ratio (P/Δ) will be used to represent the indentation stiffness. To analyse the influence of the effects of Poisson's ratios and embedment on the indentation stiffness, the ratio between the indentation stiffness for a model with an embedment and that for a homogenous material is defined as the "Indentation Stiffness Ratio". For the model with an embedded layer, the indentation stiffness ratio could be represented in the form of dimensionless formula ($\frac{P(1-v)}{4\mu\Delta b}$), where 'μ' is the shear modulus of the matrix. The formula can be obtained following an integral transform technique [4]. Briefly, in the mathematical procedure, a Hankel transformation is used to solve the governing partial differential equation for themixed boundary conditions of the matrix and the embedded layer. The dual integral equation for the region in contact with the indenter and the outside region consists of a single unknown function which can be represented by a finite Fourier cosine transform. The mixed boundary value problem was reduced to the solution of a Fredholm integral equation of the second-kind (i.e. no closed form solution), which is solved numerically in Matlab (Matlab 9.0, The MathWorks Inc., Natick, MA, 2016) following the procedure in Sneddon [40] by fitting the N values [41]. The numerical solution of the integral equations provides results that illustrate the influence of the depth of embedment of the reinforcing membrane and Poisson's ratio of the matrix material on the indentation stiffness. A N=5 was used for the numerical solution, which provided sufficiently repeatable results, further details of the mathematcial procedure and numerical implication can be found in [41].

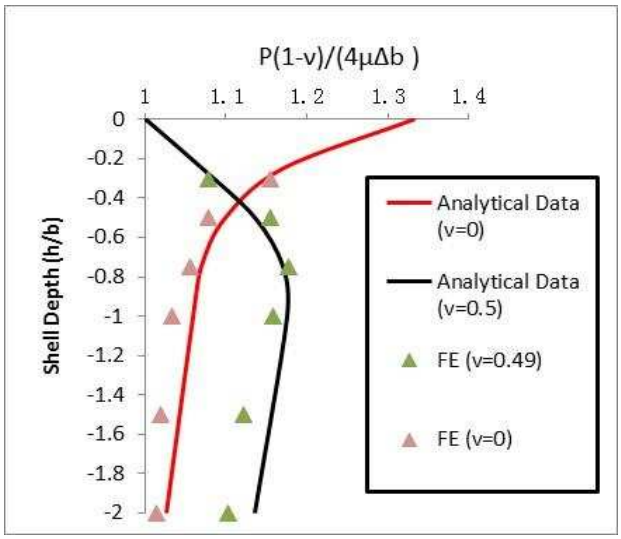

Figure 4 Comparison between the numerical and analytical data for the Indentation stiffness ratio (Sample with embedment vs. Sample without embedment).

Figure 4 is a typcial set of data from the mathematcial approach and the FE modelling (thickness of the embedded layer is 0.1mm, E_m=3MPa; E_s=300 MPa, Poisson's ratio is 0.3). As shown in the Figure, the value for $\frac{P(1-v)}{4\mu\Delta b}$ varies with the depth of the embedment as represented by the ratio of the depth (h) and the indenter radius (b). Both of the analytical results and the FE data show that, when the embedment is closer to the surface (i.e. lower h/b), the indentation stiffness ratio is higher than 1. When the shell is deeper (i.e. higher h/b), the indentation stiffness ratio is closer to 1, in other words, the embedment has less effect on the indentation resistance. As shown in the figure, the FE data is in a good agreement with the mathematically determined data. These validation data, together with results for other different properties, indicate that the FE modelling approach is sufficiently accurate for addressing the problem.

3 Results and discussion

3.1 Effect of the matrix Poisson's ratio on the deformation and indentation stiffness of embedded systems with different shell depths.

Figures 5&6 illustrate the predicted FE indentation stiffness ratio for materials with different layer embedment depth (h) and matrix Poisson's ratios. The data in Figure 5 is for an indenter radius of 1mm, while the data in Figure 6 is for an indenter radius of 2mm. The change of the indenter size naturally generates different relative depths (h/b). The thickness of the shell for the data presented is 0.1mm.

As shown by the data in Figure 5, the change of indentation stiffness ratio with the embedment depth follows a similar trend for Poisson's ratio of 0 and 0.3 (representing conditions where the material is compressible). When the shell is close to the top sample surface (h=0), the indentation stiffness ratio shows the maximum value, representing more significant effects of the stiffer layer on the indentation resistance, which is reasonable. By increasing the shell depth, the indentation stiffness ratio reduces and eventually becomes less significant. In the

cases with the Poisson's ratio being 0.4 or 0.5 (representing conditions where the material is less compressible or close to incompressible), the relationship between indentation stiffness with the layer depth exhibits a different trend. For Poisson ratio of 0.4, the indentation stiffness ratio reaches a value close to 1, at the surface (h/b close to 0), with a slight increase observed when the shell is immediately underneath the surface. When the material is incompressible (Poisson's ratio=0.5), the indentation stiffness ratio become close to 1, then increase with the layer depth and reach a peak value when h/b is about 0.75. As shown in the curves for ν=-0.3 and -0.49, the indentation stiffness ratio increased further from the data for Poisson's ratio of 0. As shown by the dotted lines in the figure, when the Poisson's ratio is negative, the indentation stiffness ratio continues to increase as the Poisson's ratio changes from 0 to a progressively more negative value. The increase of the indentation stiffness could be over 30% when the layer is very close to the surface. The presented data clearly reveals that the auxeticity of the matrix has direct influence on the indentation resistance change associated with an embedded layer.

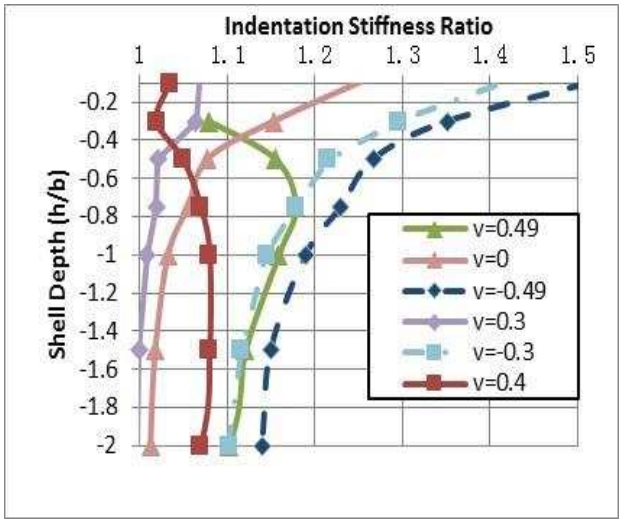

Figure 5 Numerical data showing the indentation stiffness ratio over different shell depth (represented by h/b) for different matrix Poisson's ratio. (shell thickness=0.1mm, E_s=300MPa, E_m=3MPa.

Similar data have been obtained for situations with larger indenter sizes. Figure 6 shows typical data for an indenter radius of 2mm. The effect of Poisson's ratio of the matrix on the relationship between indentation stiffness ratio and layer depth is similar to that for indenter radius of 1mm, but the indentation stiffness ratio is slightly lower. These confirm that the negative Poisson's ratio of the matrix could effectively enhance the contribution of the embedded layer to the indentation resistance of the matrix and embedded layer system, the magnitude of the effects is strongly influenced by the depth of the buried layer.

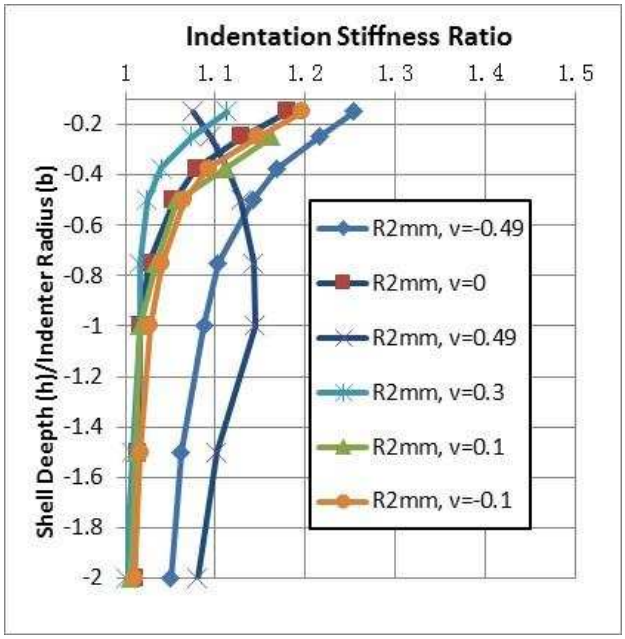

Figure 6 Indentation stiffness ratio for a larger indenter size.

3.2 Effect of the properties and dimensions of the embedded layer.

To investigate the effect of changing the properties of the embedment on the indentation stiffness, the Poisson's ratio, the stiffness and thickness of the embedded layer were varied systematically. It is essential to assess the effect of the Poisson's ratio of the layer, as potentially the effect of the auxeticity may be associated with the mismatch of the Poisson's ratio, which has been observed in other systems, such as semi-auxetic laminates or composites using a combination of materials with positive and negative Poisson's ratio [19, 25]. As shown in Figure 7, when the Poisson's ratio of the embedment changes, the indentation stiffness ratios of the materials show very limited change for a sample with a thin shell (0.1mm thickness). A similar trend is observed with other settings of different layer depth. This suggest that the enhanced indentation stiffness ratio with a matrix of a negative Poisson's ratio is unlikely to be due to mismatch of the Poisson's ratio between the embedded layer and the matrix.

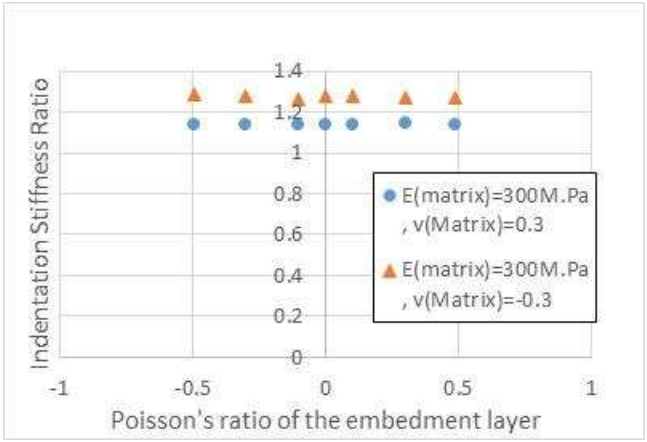

Figure 7 Effect of the Poisson's ratio of the embedment.

Figure 8 illustrates typical data regarding to the effect of the stiffness of the embedment on the indentation stiffness ratio when the layer (0.1mm in thick) is positioned at a depth of 0.5mm. The stiffness of the embedment is varied from 3 to 3000MPa, representing a normalised stiffness against the matrix (E=3MPa) of 1 to 1000. As shown in the figure, when the layer has the same stiffness as the matrix, the indentation stiffness ratio for positive and negative matrix Poisson's ratio is very close to 1, i.e. resembling a situation for indenting the matrix only. When the stiffness of the layer increases, the data for the negative Poisson's ratio matrix increases, particularly in the region when the E_s/E_m is lower than 100. Beyond this point, the increase of indentation stiffness roughly follows a linear trend but with a much lower rate in both the positive and negative matrix Poisson's ratio domains. Similar work has been conducted on layers with different Poisson's ratios for both stiff shells (E_s/E_m over 1000) and softer shells (E_s/E_m less than 10). The results show no significant difference in the trend of the effect of layer stiffness on the indentation stiffness ratio.

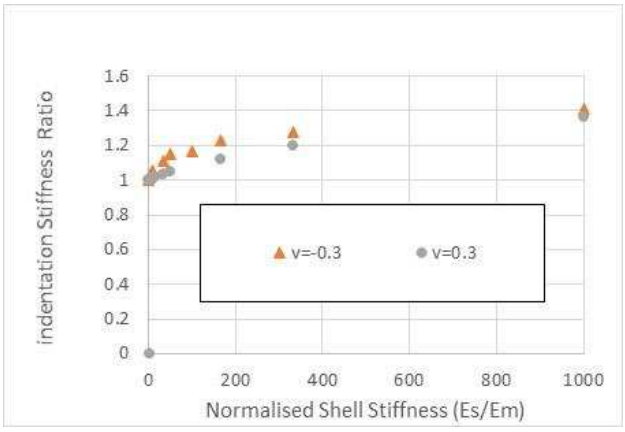

Figure 8 Indentation stiffness data showing the effect of the shell stiffness.

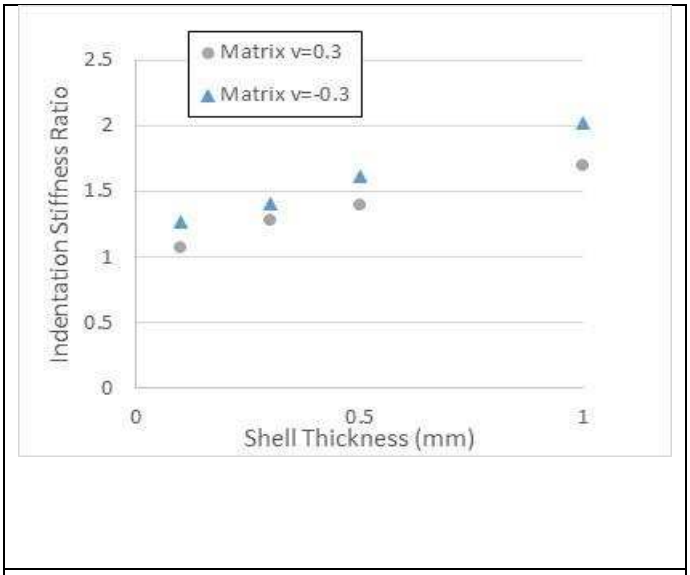

Figure 9 Effect of shell thickness on the indentation stiffness ratio.

Figure 9 is a typical set of data (h/b=0.5) showing the effect of the thickness of the embedment on the indentation stiffness ratio. This is another important factor. In real applications, the thickness of the shell could be as thin as 0.01 to 1mm for different embedded systems [1-3]. This was investigated by systematically varying the thickness of the embedment in the model. For both positive and negative matrix Poisson's ratio, the indentation stiffness of the system increased with the shell thickness. It was noted that there is no major difference in the trend of the indentation stiffness against the layer thickness between situation when the matrix is with a positive or a negative Poisson's ratio.

4 Discussion

Soft elastic materials with embedded stiffer layers are increasingly used in the medical and sports engineering fields. The validation and investigated results show that the modelling technique, with the **embedded region** function, is reliable in investigating the effect of embedded system with the freedom of changing key dimensional parameters (such as thickness) without altering the meshing elements, etc. The validated results for the homogenous sample and sample with an embedment of same properties, show a good agreement with data from the analytical solution. The comparison between the indentation stiffness ratios (enhancement parameters) also show a good agreement with the results based on an analytical approach for situations with different embedment depths. Figure 10 shows the indentation stiffness ratio from the analytical solution [4] and the FE data of this work when the stiffer layer is on top of the sample. In general, these two sets of data show a similar trend. When the material is close to incompressible (v=0.5), the embedment has limited influence on the indentation resistance. Over the positive Poisson's ratio range, the numerical data match the analytical solution very closely, which further confirms that the FE modelling approach is reasonably accurate. However, over the negative Poisson's ratio range, the FE data is slightly lower than the analytical solution. The exact reason is subject to further studies. One particular reason might be due to the interaction between the shell and the matrix. The analytical solution assume full inextensible behaviour for the embedment, this assumption may become not fully valid any more for some conditions. The data presented, from this work, clearly confirm that the matrix auxeticity has a profound effect on the mechanical behaviour of the material system, especially when the shell is on the surface or close to the surface.

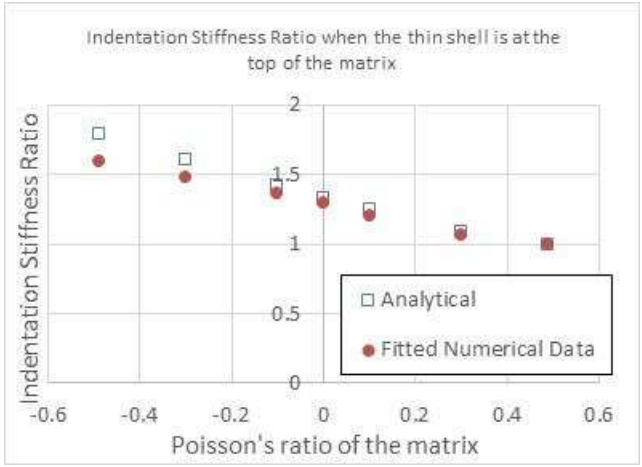

Figure 10 Comparison between the indentation stiffness ratio predicted by FE and mathematical approach.

For an embedded shell system, both the embedment and the auxeticity of the matrix influence the indentation resistance. For a flat-ended indenter over small displacement, the effect of negative or positive Poisson's ratio, for a homogenous material, is not very significant. As shown in Equation 1, a material with a Poisson's ratio of the same absolute value but opposite sign (negative or positive) would have a similar indentation stiffness. The results in this work clearly suggest that, with the embedment of thin layer close to the surface, the influence of the auxticity in the matrix becomes significant as shown in Figures 5, 6, 10. The reason for this enhanced effect of auxeticity with embedded layer is subject to further study. One potential reason might be the mismatch of the Poisson's ratio, which has been found in auxetic composite [22, 27]. For a composite material, according to [27], when positive and negative Poisson's ratio materials are used in a semi-auxetic laminate, both the in-plane and the out of plane stiffness can be increased. However, for the case of indentation on sample with embedment layer, the Poisson's ratio of the embedment showed no major influence as illustrated in Figure 8. Similar trends have been observed in a range of different combination of embedment depth and layer properties. This limited effect of the Poisson's ratio of the embedment on the indentation stiffness ratio is probably due to the fact that under indentation, the lateral deformation of the embedded layer is rather limited due to its high stiffness and possible restraints from the matrix. This suggest that the Poisson's ratio mismatch is not the main reason for the effect of auxeticity on the indentation stiffness increase.

As shown in Figure 8, the effect of the stiffness of the embedment on the indentation stiffness ratio follows a different trend over different stiffness ranges. When the embedded layer has a relatively low stiffness value, the indentation resistance increases with layer stiffness more significantly. With higher stiffness values for the embedment layer, a linear relationship is observed between the stiffness of the layer and the indentation stiffness ratio. Similarly, a linear relationship is found between the thickness of embedded layer and the indentation stiffness ratio (Figure 9), which is similar to the case for a free standing membrane with fixed boundary conditions [38].

Apart from the influence of auxeticity on the indentation resistance ratio, the deformation and stresses of the embedment, is also important, as it may influence the function of the embedment.

Figure 11 compares the displacement fields (a-c) and maximum principal in-plane stresses of the embedded layer (d) between matrix with positive and negative Poisson's ratios. As shown in the Figure, the overall deformation of the embedment (a-c) is similar but there is a difference in the distribution of the maximum in-plane principal stress (d). Figure 11(c) plots detailed profile of the vertical displacement along the radial direction. As shown in the curves, with a negative Poisson's ratio for the matrix, the maximum displacement is slightly less than the displacement with a positive Poisson's ratio, but the region outside the sample-indenter contact area exhibits a higher displacement. This suggests a larger volume of material potentially has been involved in the deformation for the region under the embedment. Figure 11(d) plots the profile of in-plane maximum principal stresses along the radial direction for matrix Poisson's ratio of 0.49, -0.49, 0.3 and -0.3. As shown in the curves, for a positive matrix Poisson's ratio, the stress in the section underneath the indenter is predominantly positive, which signifies that the principal direction is outward from the indenter. On the other hand, the maximum in-plane stress in the layer underneath the indenter for the negative Poisson's ratio matrix is negative, implying a strong inward force and the material is being dragged in. This result is consistent with the difference between the auxetic and non-auxetic materials under indentation. For a nonauxetic material, the material tends to be pushed away, this causes tension radially in the thin layer. For the auxetic material, it tends to draw in towards the indenter causing compression mode of loading on the thin embedded layer. The involvement of the embedment in such as process is likely to increase the effective indentation resistance. Further studies are required to investigate these issues.

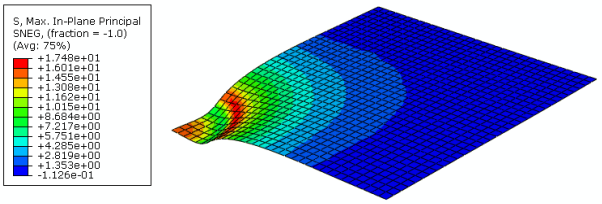

(a) Deformed shape and distribution of the maximum in-plane stresss.

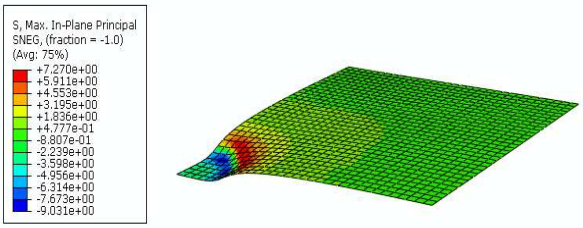

(b) Deformed shape and distribution of the maximum in-plane principal stress.

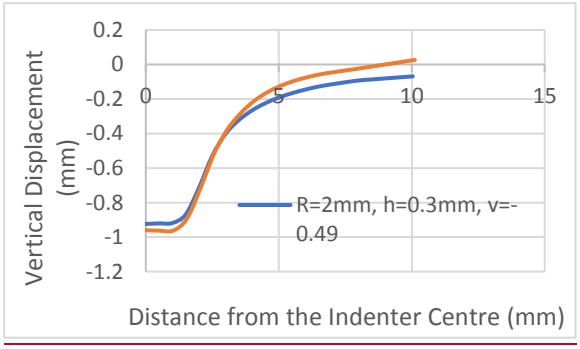

(c) Profile of the vertical displacement of the embedment layer.

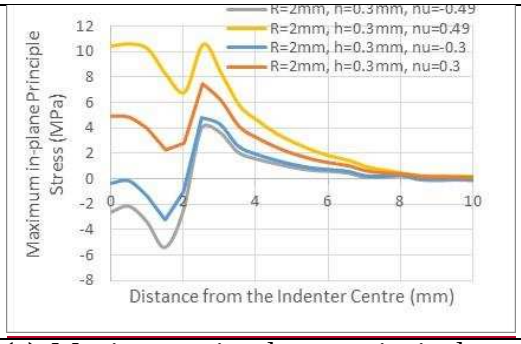

(c) Maximum in-plane principal stress along the radial direction. .

Figure 11 Comparison of the deformation and the maximum in-plane principal stress of the embedment between materials with a matrix of a positive or negative Poisson's ratio.

5 Conclusions

In this work, the deformation of a soft material with an embedded stiffer layer under cylindrical flat indenter was investigated through FE modelling. A practical approach in modelling embedded system is evaluated and presented. The FE results are correlated with an analytical solution for homogenous materials and results from an mathematical approach for embedded systems in a half space. The indentation stiffness/resistance of soft material systems with embedded thin layer under flat-ended indenter for matrix of both positive and negative Poisson's ratio values were systematically studied. The influence of auxeticity on the indentation stiffness ratio and the deformation of the embedded system under different conditions (indenter size, thickness and embedment depth of the embedded layer) was established and key mechanisms of the Poisson's ratio effect are highlighted. The results show that the auxeticity of the matrix has a direct influence on the indentation stiffness of the system with an embedded layer. When the embedment is close to or on the surface of a matrix, with a high positive Poisson's ratio (e.g. 0.5), the shell has limited effect on the indentation resistance. The enhancement of indentation resistance due to embedment increases, as the matrix Poisson's ratio is decreased to zero and to negative values. The indentation stiffness could be increased by over 30% with a thin inextensible shell on top of a negative Poisson's ratio matrix. The deformation of the embedded layer is significantly influenced by the auxeticity of the matrix. With a non-auxetic matrix, the embedded layer underneath the indenter is being pulled, while for auxetic matrix, the embedded layer is being pushed due to the combined influence of the deformation of the auxetic matrix.

References

[1] K. Harmeyer, M. A. Holland, and G. Krutz, Strain **45**, 543 (2009).
[2] G. Cannata and M. Maggiali, An Embedded Tactile and Force Sensor for Robotic Manipulation and Grasping, Robotics Research, in Proceeding of the 16th Int. Symposium Robotic Research (ISRR). edited by M. Inaba and P. Corke (Springer, Berlin, 2016).
[3] S. C. Shit and P. Shah, Natl. Acad. Sci. Lett. **36**(4), 355 (2013).
[4] A.P.S. Selvadurai, Int. J. Eng. Sci. **47**(11), 1339 (2009).
[5] M. Rahman andG. Newaz, Int. J. Eng. Sci. **35**, 603 (1997).
[6] V.I. Fabrikant, Arch. Appl. Mech. **81**(7), 957 (2011).
[7] M. Eskandari, H. M. Shodja, and S. F. Ahmadi, Eur. J. Mech. A/Solids **39**, 134 (2013).
[8] H. M.Shodja, S. F. Ahmadi, and M. Eskandari, 2014, Appl. Math. Modell.**38**, 2163 (2014).

[9] M. Kalantari, A. Khojasteh, H. Mohammadnezhad, M. Rahimian, and R. Y. S. Pak, Int. J. Eng. Sci. **91**, 34 (2015).
[10] K. W. Wojciechowski, J. Phys. A Math. Gen. **36** (,11), 765(2003).
[11] N. Gasper, X. Ren, C. W. Smith, J. N. Grima, and K. E. Evans, Acta Mater. **53**(8), 2439 (2005).
[12] J. N. Grima, R. Cauchi, R. Gatt, and D. Attard, Composite Strut. **106**, 150 (2013).
[13] M. Sanamia, N. Raviralaa, K. Aldersona, and A. Alderson, Procedia Eng. **72**, 453(2014).
[14] C.S. Ha, M. E. Plesha, and R. S. Lakes, Phys. Status Solidi B **253**(7), 1243 (2016).
[15] M. Bilski and K.W. Wojciechowski , Phys. Status Solidi B **253**, 1318 (2016).
[16] R. S. Lakes, Science **235**, 1038 (1987).
[17] R. F. Almgren, J.Elast., **15**, 427 (1985).
[18] K. W. Wojciechowski, Mol. Phy.**61**, 1247 (1987).
[19] H. Jopek and T. Strek, Phys. Status Solidi B **252**(7), 1551 (2016).
[20] G. W. Milton, J. Mech. Phy. Solids **40**, 1105 (1992).
[21] J.C.A. Elipe and A.D. Lantada, Smart Mater. Struct. **21**(10), 105004 (2012).
[22] K.W. Wojciechowski, F. Scarpa, J. N. Grima, and A. Alderson, Phys. Status Solidi B**253,** 1241(2016).
[23] A. A., Pozniak, A. Artur, K. W. Wojciechowski, J. N. Grima, and L. Mizzi, Compos Part B **94**, 379 (2016).
[24] T. Strek, H. Jopek, and M. Nienartowicz, Phys. Status Solidi B **252**,1540 (2015).
[25] T. Strek, H. Jopek, and E. Idczak, Phys. Status Solidi B **253** (7), 1387 (2016).
[26] T. Strek H. Jopek, and K.W. Wojciechowski, Smart Mater. Struct. **25**, 054002 (2016).
[27] K. K. Saxena, R. Das, and E.P. Calius, Adv. Eng. Mater. **18**, 1847 (2016).
[28] H. M. A. Kolken, and A. A. Zadpoor, RSC Adv.**7**, 5111(2017).
[29] A. A. Pozniak and K. W. Wojciechowski, Phys. Status Solidi B **251**, 367 (2014).
[30] Y. Prawoto, Com. Mat. Sci.**58**, 140 (2012).
[31] N. Chan and K. E. Evans, J Cell Plast **34**, 231 (1998).
[32] T. C. Lim, Auxetic Materials and Structures (Springer, London, 2014).
[33] D. Photiou, N. Prastiti, E. Sarris, and G. Constantinides, Int. J. Solids Struct. **81**, 33 (2016).
[34] B. Liu, X. Feng, and S. M. Zhang, Compos. Sci. Tech. **69**, 2198 (2009).
[35] J. W. Narojczyk, M. Kowalik, and K. W. Wojciechowski, Phys. Status Solidi B **253**, 1324 (2016).
[36] H. X. Zhu, T. X. Fan, and D. Zhang, Sci.Rep. **5**(14103), 1 (2015).
[37] I. I. Argatov, R. Guinovart Díaz, and F. J. Sabina, Int. J. Eng. Sci. **54**, 42 (2012).
[38] J. Aw, H. Zhao, A. Norbury, L. Li, G. Rothwell, and X. J. Ren, Phys. Status Solid B **252**(7), 1526 (2015).
[39] Simulia Abaqus, User's Manual version 6.14, Dassault Systèmes Simulia Corp, section 15.15.8 and section 35.4.1 (embedded elements).
[40] I. N. Sneddon, Int. J. Eng. Sci. **3**, 47 (1965).
[41] S. Li, PhD Thesis, Liverpool John Moores University, UK (in process).